MIMO Antenna System for Reception and Transmission of 5G Network Signals

Gorkem Akilhoca

Submitted to the
Institute of Graduate Studies and Research
in partial fulfillment of the requirements for the degree of

Master of Science
in
Electrical and Electronic Engineering

Eastern Mediterranean University
February 2022
Gazimağusa, North Cyprus

Approval of the Institute of Graduate Studies and Research

Prof. Dr. Ali Hakan Ulusoy
Director

I certify that this thesis satisfies all the requirements as a thesis for the degree of Master of Science in Electrical and Electronic Engineering.

Assoc. Prof. Dr. Rasime Uyguroglu
Chair, Department of Electrical and Electronic Engineering

We certify that we have read this thesis and that in our opinion it is fully adequate in scope and quality as a thesis for the degree of Master of Science in Electrical and Electronic Engineering.

Assoc. Prof. Dr. Rasime Uyguroglu
Supervisor

Examining Committee

1. Prof. Dr. Hasan Amca

2. Prof. Dr. Mehmet Kusaf

3. Assoc. Prof. Dr. Rasime Uyguroglu

ABSTRACT

Evolution from 4G to 5G is a concept which is still new and not currently applied in many countries, even though we are ahead of the planned global launch of 5G network system. The base station antennas located in T.R.N.C. are set to work in 3G operations. Proposed work consists of 2 sets of antennas to be used for below 6 GHz band and at 35 GHz of the mmWave band. Sub-6 GHz antenna operates at 3.44 GHz, 2.83 GHz, 2.39 GHz, and 1.07 GHz. The components are suitable to be mounted additionally to the current base stations, making it cost effective in terms of replacing the previous antenna boxes. The modular freedom of the system makes it like jigsaw puzzle logic, easier for towers to be modified according to the demand in the given area. 5G networking will use many antenna points, these designs can be used inside substation antenna panels and antenna boxes for home use. The design was deeply studied in CST Microwave Studio, mostly utilizing the array factor format in simulation features, widely used antenna parameters were obtained and compared with suitable results. Techniques to finely tune the patch antenna were applied throughout the designs, such as partial and meandered ground, slot cutting and inset feeding, their effects are recorded during the working period. To achieve MIMO functionality, the antennas can be assigned to a port, rather than being connected to a series of same antennas altogether. In each port, a phase shifter can achieve beam steering, so that a member of the array can scan a given area. The digital signal processing was not accounted for in the work, the mechanical part of the design was thoroughly studied.

Keywords: MIMO, 5G, patch antenna.

ÖZ

4G'den 5G'ye evrim, 5G ağ sisteminin planlanan küresel lansmanından önce olmamıza rağmen, hala yeni olan ve birçok ülkede şu anda uygulanmayan bir kavramdır. K.K.T.C.'de bulunan baz istasyonu antenleri 3G operasyonlarında çalışacak şekilde ayarlanmıştır. Önerilen çalışma, 6 GHz bandının altı ve mmWave bandının 35 GHz'i için kullanılacak 2 set antenden oluşmaktadır. Sub-6 GHz anteni 3.44 GHz, 2.83 GHz, 2.39 GHz ve 1.07 GHz'de çalışır. Bileşenler, mevcut baz istasyonlarına ek olarak monte edilmeye uygundur, bu da önceki anten kutularının değiştirilmesi açısından maliyet bakımından verimli olmasını sağlar. Sistemin modüler özgürlüğü, yapboz mantığı gibi, kulelerin verilen alandaki talebe göre modifiye edilmesini kolaylaştırır. 5G ağ iletişimi birçok anten noktası kullanacak, bu tasarımlar ev kullanımı için trafo anten panelleri ve anten kutuları içinde kullanılabilir. Tasarım, simülasyon özelliklerinde çoğunlukla dizi faktör formatı kullanılarak CST Microwave Studio'da derinlemesine çalışılmış, yaygın olarak kullanılan anten parametreleri elde edilmiş ve uygun sonuçlarla karşılaştırılmıştır. Kısmi ve menderesli zemin, yarık kesme ve gömme besleme gibi tasarımlar boyunca yama anteni ince ayar teknikleri uygulandı, etkileri çalışma süresi boyunca kaydedildi. MIMO işlevselliğini elde etmek için, antenler bir dizi aynı antene tamamen bağlanmak yerine bir bağlantı noktasına atanabilir. Her bağlantı noktasında, bir faz kaydırıcı ışın yönlendirmesini gerçekleştirebilir, böylece dizinin bir üyesi belirli bir alanı tarayabilir. Çalışmada dijital sinyal işleme dikkate alınmadı, tasarımın mekanik kısmı kapsamlı bir şekilde incelendi.

Anahtar kelimeler: MIMO, 5G, Mikroşerit Yama Anten

TABLE OF CONTENTS

LIST OF TABLES

LIST OF FIGURES

LIST OF SYMBOLS AND ABBREVIATIONS

Deg	Degree
Gbps	Gigabits per Second
GHz	Gigahertz
LTE	Long Term Evolution
Mbps	Megabits per Second
MHz	Megahertz
MIMO	Multiple-input, Multiple-output

Chapter 1

INTRODUCTION

Ever-growing technological advancements create many opportunities for achieving faster, stable connections wirelessly, and there is no doubt that 5G is far more superior than its predecessor 4G, which was first used a decade ago. In addition to increase in the bands of the current LTE network, an interval called “mmWave” is allowed to be used for communication purposes. There are two sections in 5G networking. Those are sub-6 GHz levels and mmWave sections. Sub-6 covers the range of 0.4 GHz to 6 GHz whereas mmWave covers the range of 30 GHz to 300 GHz. The downside of mmWave technology is that the wavelength of the signal is so small that it can be blocked by objects such as buildings and trees. Many access points should be thought carefully and constructed such that coverage problem is overcome. Sub-6 GHz frequencies does not suffer from this phenomenon. 3G provides up to 10 Mbps, 4G provides up to 100 Mbps, and 5G is planned to provide at least 20 Gbps, which is 2000 and 200 times faster than the past two predecessors. The key feature to obtain this great increase in speed is MIMO technology. Each member of the antenna array is treated as a single entity, transmitting, and receiving the signals within the same radio channel. By doing so, a concept called antenna diversity is achieved. It increases the quality of a signal and strengthens the connection. While the antennas are connected individually for diversity property, another setting in the antenna radiation called beam steering can be utilized too. Addition of phase shifters to each antenna port, magnitude and phase can be set for a particular antenna. Change in the magnitude and the phase of the signal

allows the radiation pattern to be directed to a certain angle. This effect can also be achieved by adjusting the lengths of the transmission lines, but that would result in more antennas connected to each other and decrease in MIMO capacity.

Microstrip patch antennas are used for these types of applications, due to them being fabricated at low costs, and being versatile enough to be almost used in everyday electronic devices ranging from handheld equipment to large scale broadcast towers. A single antenna can resonate at certain frequencies, a design challenge which includes taking certain shapes from the copper patch. By doing so, strength of the resonating signal can increase, bandwidth of the resonance can increase, and additional resonating signals can be observed near the resonant frequency of the designed patch, making it a multiband antenna.

To understand what has done in previous works by other people, wide range of articles, seminars and symposiums are reviewed extensively. A paper [1] relatively close to the subject was found and studied in CST software. The designs were copied and tested virtually, and confirmation of similar results were obtained. In that paper, a four-element antenna was used under a radome cap for a base station. Another design [2] that included reflector panels to increase the bandwidth of the signals. To combine several patches together with different feeding techniques, [3] was followed and tested virtually again. The topic on transmission line transformers were studied in [4], and yet again tests were carried out on the subject.

1.1 Thesis Objective

The aim of the project is to design a system that can facilitate both sub-6 GHz and mmWave signals in 5G spectrum.

1.2 Thesis Contribution

Modular concept of the project allows the engineers to create arrays according to their own design patterns. By using array formatting in simulation environments, phases magnitudes and antenna member distances can be set to achieve desired gain and radiation pattern.

1.3 Thesis Format

Chapter 1 is the brief explanation of the project. Chapter 2 contains theoretical information about antennas in general. Chapter 3 revolves around patch antennas, how and in what ways they can be used, modifications which can be applied, and their effects on the antenna parameters. Chapter 4 is the section which specifies the design parameters and the results of the proposed work with comments. Chapter 5 ends the thesis with a conclusion section, and what can be done in the future.

Chapter 2

ANTENNAS

2.1 Antenna

An antenna is portrayed as a transformer which converts electrical signals into electromagnetic waves [5]. All antennas can and do operate in two modes, receiving or transmitting antenna. If an antenna is in reception state, it accepts the signal and turns it into current. If the antenna is in transmission mode, it radiates electromagnetic waves, due to current applied to it. This can be achieved by connecting the conductor/radiator with a computerized power source, which generates, or reads the signal to be used by the antenna. Below this heading, some theoretical parameters are explained revolving around the context of this thesis.

2.2 Antenna Parameters

For determining optimal operating conditions for an antenna, several criteria are investigated when testing. These values must satisfy a standard to ensure all working conditions are set accordingly.

2.2.1 S11/Return Loss

Return loss is defined by the ratio of transmitted energy with respect to input energy. For an acceptable antenna, the usual value for a certain frequency is to be at least –10 dB. It corresponds to 90% of the input power being transmitted, and 10% is dissipated along the conducting material. Increase in “10” in dB scale, corresponds to 10 times increase in the previous value. To give an example about this, -20 dB results in 99% of the input power being transmitted.

$$RL = 10log_{10}\left(\frac{P_{in}}{P_{out}}\right) dB \qquad [6]$$

where P_{in} is input power and P_{out} is the power radiated from the antenna.

2.2.2 Voltage Standing Wave Ratio

VSWR value a quite like the previous parameter. In this context, it is the ratio of applied voltage to the antenna to returned voltage from the antenna read by the source. A general rule states that value of 2 is acceptable in many antenna applications. Less than 2 VSWR means the source and the antenna is nearing perfectly matched. Due to being a ratio, VSWR has no units or whatsoever.

$$VSWR = \frac{(1+|\Gamma|)}{(1-|\Gamma|)} \qquad [7]$$

where Γ is the reflection coefficient.

2.2.3 Impedance

Impedance of the antenna system is measured from the connection ports of the individual, or series of antennas. The usual impedance value looked for is 50Ω. This is due to mean between two values of impedances used in coaxial cables. 30Ω handles the power very well, while 77Ω has the lowest power loss. Almost all cable connectors are manufactured to 50Ω impedance. Impedance matching is critical, as mismatch imbalances the 1:1 power transmission, decreasing the efficiency of the antenna.

$$\Gamma_{11} = \frac{Z_2+Z_1}{Z_2-Z_1} \qquad [8]$$

where Γ_{11} is the return loss, and Z_2 and Z_1 are the load and antenna impedances respectively.

2.2.4 Efficiency

Antenna efficiency is a value that is a ratio of power transmitted to the input and power generated in the source. Due to losses in material medium, heat generation, some of

the energy becomes waste products, resulting in less power transfer to the working structure. Thus, achieving 100% efficient antenna is not technically feasible.

$$\eta = \frac{P_{out}}{P_{in}} * 100$$

where η is efficiency, P_{out} is the output power, and P_{in} is the input power of the antenna. Multiplication by 100 to get the percentage value.

2.2.5 Bandwidth

Bandwidth of the frequency transmitted or received by the antenna is determined by observing the minimum and maximum value that corresponds to the –10 dB scale in return loss graph. Having a range of freedom despite being designed to radiate at a resonant frequency, this way antennas allow tolerance in shifts occurring in frequency while operating near perfect condition.

2.2.6 Radiation Pattern

Radiation pattern is the 2D or 3D representation of an antennas' power transmission at certain angles in electromagnetic planes. Electric and magnetic planes are the medium of wave propagation; thus, the intensity of signal varies according to the change in degree from origin. Planes are orthogonal to each other, meaning they have 90 degrees rotation in between them. Information is carried by two of these planes, due to them having a nature of dependency on each other. Variation in one plane is mimicked on the other.

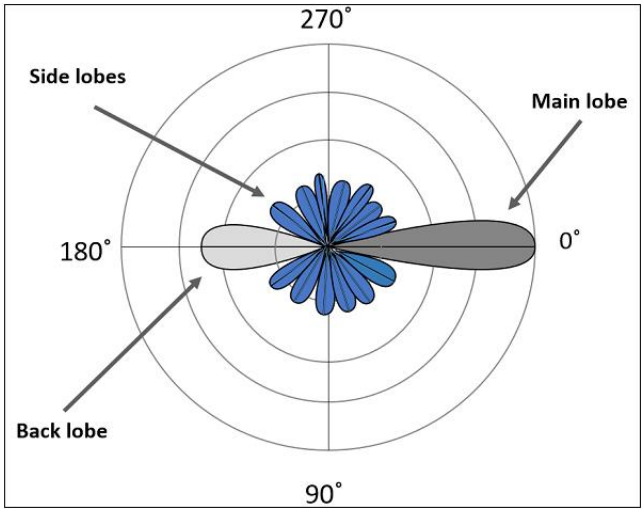

Figure 1: Radiation pattern of an antenna [9].

2.2.7 Directivity

Directivity of an antenna is calculated by dividing the radiation intensity from a point by the total radiation intensity averaged in all directions. It is a measure of how well the antenna directs the signal towards a certain direction. It is measured in decibel scale.

$$D = \frac{4\pi U}{P_{rad}} \qquad [10]$$

where U is the radiation intensity and P_{rad} is the total power radiated.

2.2.8 Gain

Gain has a relationship with directivity, as it is calculated from it. Gain takes the efficiency of the antenna additionally. Only difference between directivity is that, instead of having total power radiated from the antenna, gain uses the total power input to the antenna.

$$G = \eta * D \qquad [10]$$

Where η is the efficiency of the antenna and D is the directivity of the antenna.

2.2.9 Polarization

Polarization is the orientation of electromagnetic waves in the propagation medium. There are several configurations of polarizations suited for each unique application. For instance, circular polarized signals excel at penetrating buildings better than linear polarized signals.

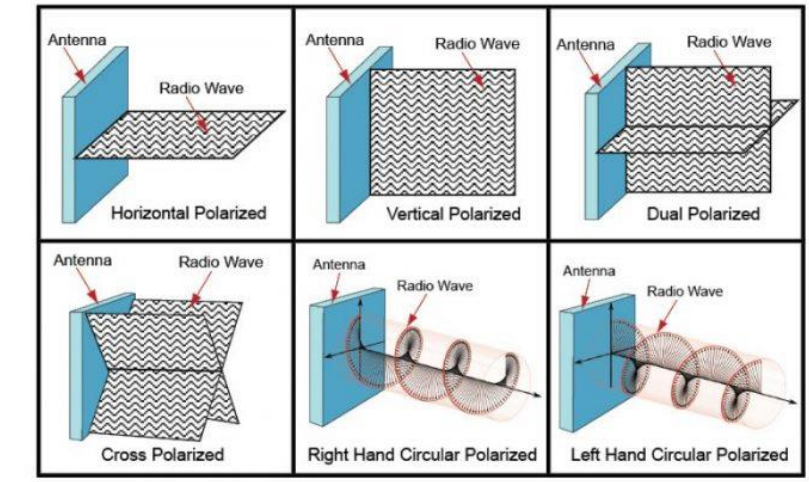

Figure 2: Types of antenna polarizations [11].

2.2.10 Beamwidth

Beamwidth is the angle of the main lobe of the radiation pattern, that the lobe decreases half the power, roughly -3 dB. It can be used to determine how wide the antenna can scan the given space.

2.3 Antenna Configurations

To boost the several parameters mentioned above, antennas are modified mechanically. Mounting them side by side, stacking them on top of each other, or fabricating many antennas in x-y plane on the same working plane creates an array formation.

2.3.1 Array Antennas

A few advantages of using antennas in multiples include an increase in signal strength, increase in directivity, and increase in gain [2]. By combining and increasing ports on the connection terminals radiation pattern of the entire system changes. To achieve this “beam steering” technique, changes in the signal phase must be applied on stated ports.

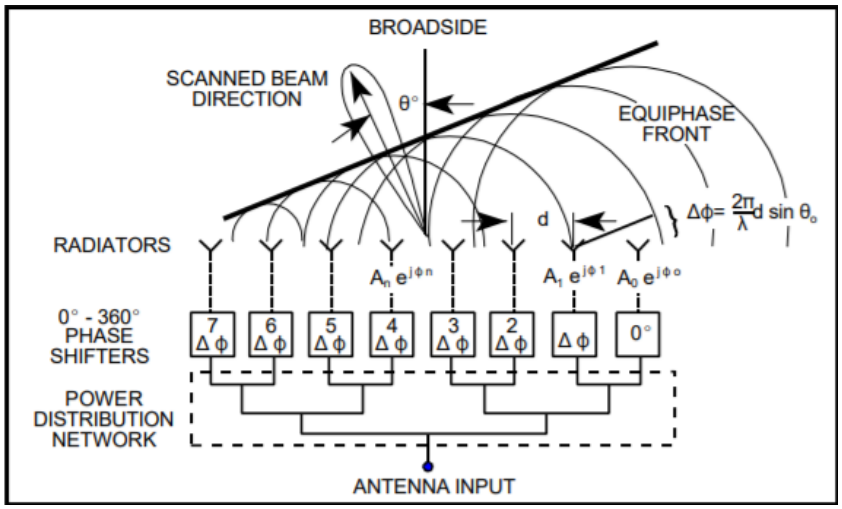

Figure 3: An example of beam steering by using phase shifters [12].

This technique is used in radar applications, and for communication-wise it is being employed to achieve coverage through the medium.

2.3.2 MIMO

The multiple-input multiple-output technology exploits the usage of many antennas to transmit and receive signals over a vast amount of signal paths to strengthen the connection and reducing fading of the signal. The signals reach to their destination more easily, as the signals can scatter around the buildings in cities. Adopting several antennas increases the coverage of the transmission of the antenna system.

MIMO systems divide the signal to individual elements before transmission, that way a string of information can be received at the end and recombined to make the initial information at greater speeds [14].

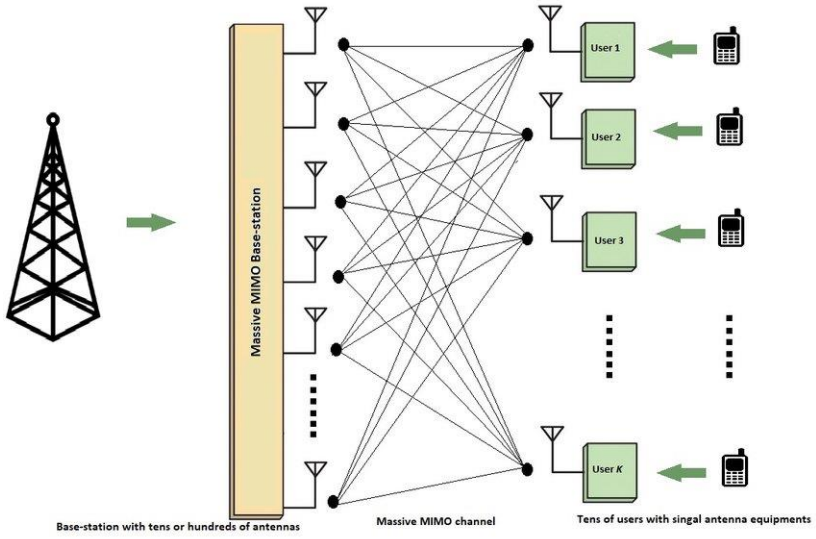

Figure 4: A basic representation of MIMO system [13].

Chapter 3

PATCH ANTENNAS

3.1 Patch Antenna

A patch antenna is a system which consists of three layers. These are the bottom conducting material, which is defined as the ground, the middle dielectric layer, and the top layer which consists of a radiating patch and usually transmission lines. Not all the patch antennas require transmission lines to be fed from.

Radiation occurs at the edges of the conducting patch at the top layer and the ground plane, causing a phenomenon called fringing fields. The electric field is present throughout the patch. The addition of phases of the field lines which creates the fringing fields at the edges of the patch creates the radiation pattern.

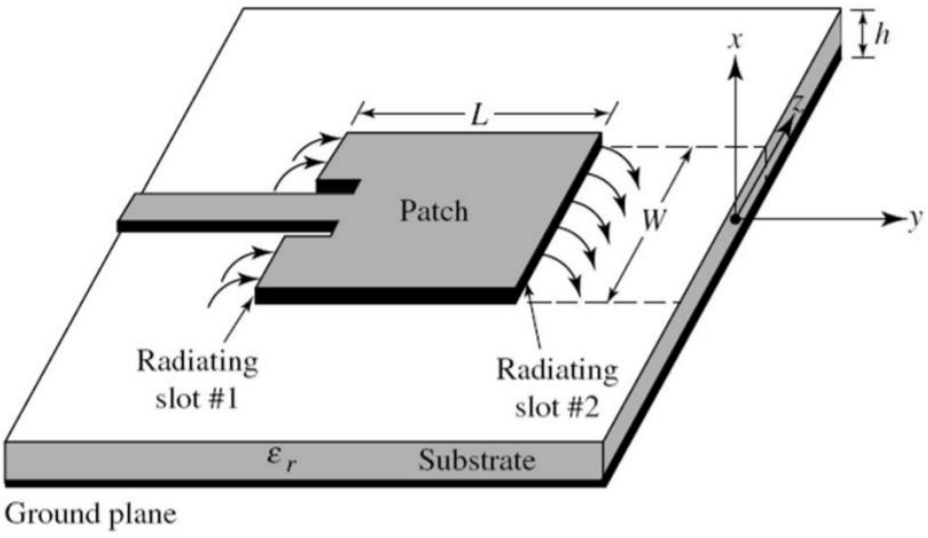

Figure 5: Fringing fields shown near the edges [15].

Main uses of the patch antennas usually take place in the microwave region, where the wavelengths of the signals are short enough, and easily picked by small sized patches. Fabrication of the patch antennas is easy and low cost; thus, they are used in portable devices such as cell phones. Their power strengthens as the number of antennas increases in a system, which was mentioned in the previous chapter.

3.2 Modifications on the Patch Antenna

To finely tune the patch antenna, several pieces can be added or removed from the ground plane or the radiating patch. In the next headings, modification types and their effects observed on the antenna will be discussed.

There are mathematical expressions to represent the effects of the modifications on the patch antenna, but instead of studying the theoretical meanings and their outcomes, trial and error method was used to determine the effects on the system in CST environment. The final design is the product of such a technique, as the previous versions of the design were studied and kept for reference. For comparison, the screenshots of the previous versions will be available in appendices section.

3.2.1 Width and Length of the Patch

The width and length of the patch antenna is determined by the center frequency that is designed to operate. The equations to find out the dimensions are calculated using the equations below.

$$Width = \frac{c}{2f_0\sqrt{\frac{\varepsilon_R+1}{2}}} \quad [16]$$

$$\varepsilon_{eff} = \frac{\varepsilon_R+1}{2} + \frac{\varepsilon_R-1}{2}\left[\frac{1}{\sqrt{1+12\left(\frac{h}{W}\right)}}\right] \quad [16]$$

$$Length = \frac{c}{2f_0\sqrt{\varepsilon_{eff}}} - 0.824h\left(\frac{\left(\varepsilon_{eff}+0.3\right)\left(\frac{W}{h}+0.264\right)}{\left(\varepsilon_{eff}-0.258\right)\left(\frac{W}{h}+0.8\right)}\right) \quad [16]$$

where c is the speed of light, ε_R is the dielectric constant, ε_{eff} is the effective permittivity, f_0 is the center frequency and h is the height of the substrate.

By changing the dimensions of width and length, the center frequency shifts accordingly.

3.2.2 Cutting Slots in the Ground Plane

By removing some of the ground plane, a shift in the resonant frequency is observed towards lower frequencies [17]. The bandwidth and the gain of the antenna are not affected critically.

3.2.3 Cutting Slots in the Patch

Just like removing a piece from the ground plane, a reduction in patch results in a little shift in frequency towards lower frequency, but it drastically changes the resonant frequencies' return loss values. Some of the resonant frequencies suffered from decrease in return loss, while some gained an increase in the S11 graphs.

3.2.4 Miter Bend

By introducing a cut to the corner of the transmission line, characteristic impedance of the line is restored as the chopped part decreases capacitance [18]. To equalize some of the return loss values, miter bend technique is applied to the transmission line.

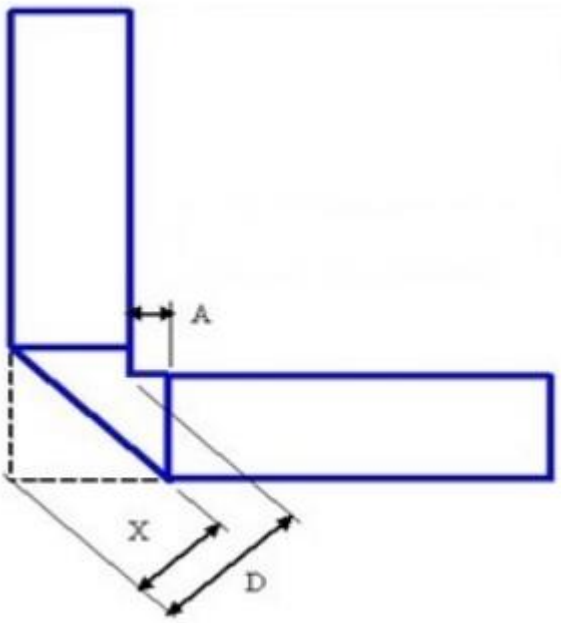

Figure 6: Illustration of a miter bend with dimensions [19].

$$D = W * \sqrt{2} \quad [19]$$

$$X = D * (0.52 + 0.65e^{\left(-1.35*\left(\frac{W}{h}\right)\right)}) \quad [19]$$

$$A = \left(X - \frac{D}{2}\right) * \sqrt{2} \quad [19]$$

3.2.5 Partial Ground Plane

Using partial ground plane in the design increases the ratio between front lobe and back lobe, meaning that most of the radiated signal travels in forward direction. It also decreases the mutual coupling generated between several antennas placed together [20].

3.2.6 Meandered Ground Plane

Like partial ground, meandered sections of the ground plane are a path that looks like a labyrinth with various dimensions cut away from the ground. The advantage of having them in the design is that they dramatically remove the mutual coupling in between elements placed near each other.

Chapter 4

DESIGN, SIMULATION AND COMMENTS

4.1 The Design of the Proposed Antennas

Here below in figures, the designs of the antennas can be observed.

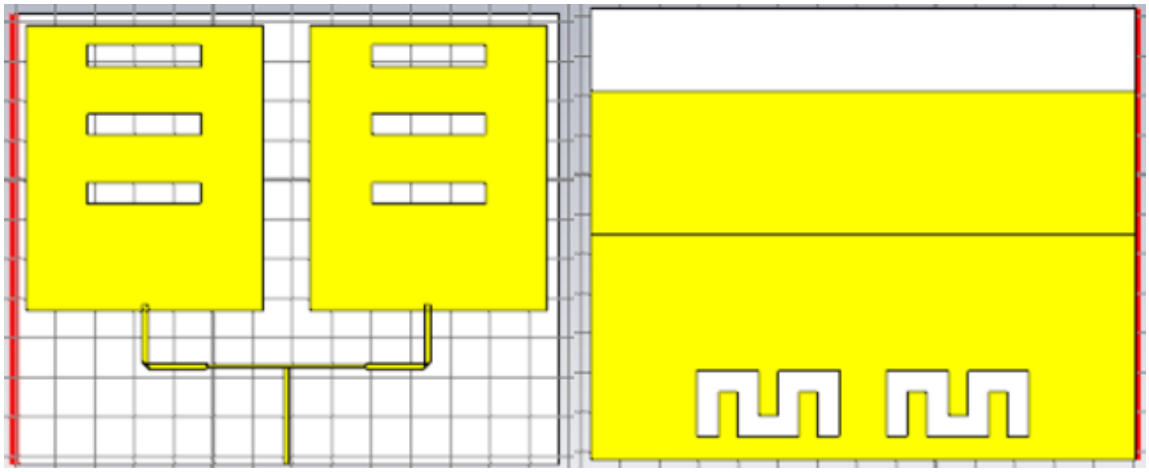

Figure 7: Design for sub-6 GHz patch antenna.

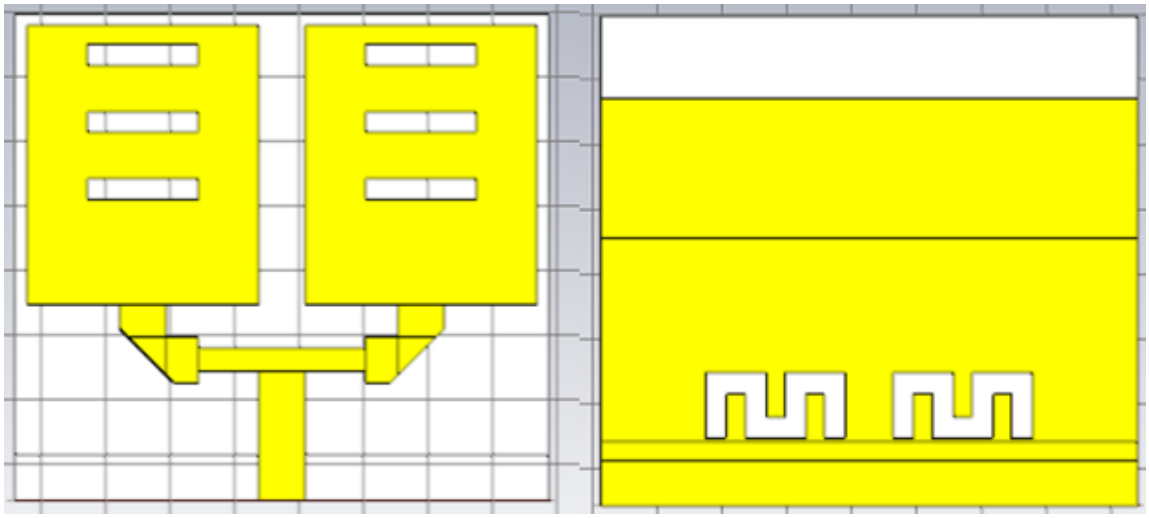

Figure 8: Design for mmWave frequency patch antenna.

The mmWave antenna is scaled down version of the first designed sub-6 GHz antenna. By utilizing the scale function of CST, values in antenna's x and y direction decreased to an allowed value. Z direction was left unchanged, as to keep consistency in conductor and substrate thickness.

Iterative adjustment method was used to finely tune both antennas. Creation started with a plain square patch antenna with no modifications and became the final product by retracing the steps carried out earlier, or by carrying out parametric sweeps to dimensions of the circuit elements. There is no mathematical way to prove what is done to make the final design. The versions of previous models are kept recorded, and they are used to aid the explanation of the general format of the project.

4.2 Sub-6 GHz Patch Antenna

The square copper patch is laid upon FR-4 material substrate, with 0.8 mm thickness and relative permittivity of 4.3. It is a two-patch system combined with a microstrip line, utilizing quarter wave power transformer to feed both antennas with one input.

4.2.1 Dimensions of Sub-6 GHz Antenna

The width and length of the patch is 60 x 72 mm, respectively. Copper is used for conductor and has thickness of 0.035 mm on both sides of the antenna. On the front side of the antenna, there are 3 slots which are 28.8 mm wide and 5.4 mm long. They are in the middle of the antenna and have 12 mm in between each slot cut. The first slot is located 4.8 mm down from the top of the antenna. The square patches have 72 mm separation, accounted from their middle face points. To ensure 50Ω impedance, 1.41 mm was found to be the width of the feeding line. Creating the T-junction in the middle of the feed, 70Ω was required, and its width is 0.75 mm.

On the back of the substrate, partial and meandered ground techniques were used. The ground plane measures 93 mm from bottom. The dimension of the meandered section is shown in the figure below. The whole shape is 5.7 mm above the bottom, and the distance between two meandered shapes is 12mm. They are center oriented.

The width and the length of the substrate is 138 mm and 114 mm.

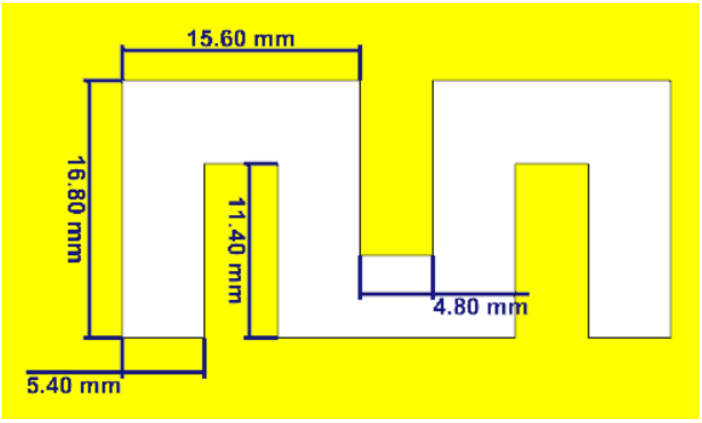

Figure 9: Dimensions of the meandered ground of sub-6 GHz.

4.2.2 Results of Sub-6 GHz Antenna

This design allows multiple resonant frequencies to be achieved. It resonates at 1.07 GHz, 2.39 GHz, 2.83 GHz, and 3.44 GHz. The last two frequencies lie on C-band, which will be used with 5G when it is commercially available.

4.2.3 S11/Return Loss of Sub-6 GHz Antenna

Here below, a graph of return loss values can be observed for this antenna. As can be seen, the maximum value of return loss is –15.9, which satisfies the minimum requirement for it to be a good transmission antenna.

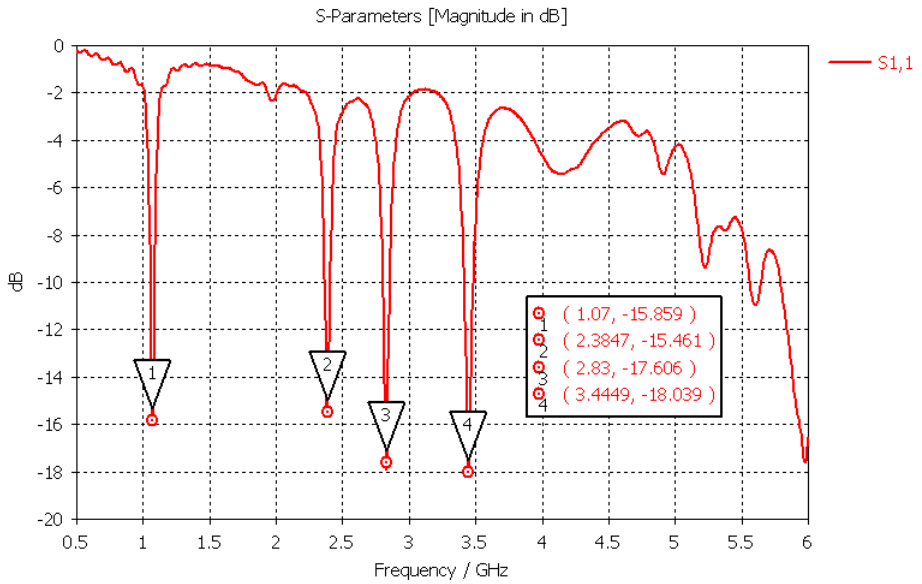

Figure 10: S11 parameters for sub-6 GHz antenna.

The bandwidth of the signals are 31 MHz, 40 MHz, 51 MHz, and 377 MHz respectively starting from the lowest resonant signals.

4.2.4 Radiation Patterns of Sub-6 GHz Antenna

Because it is a multiband antenna, patterns are different in each resonant frequency. Below in figures, radiation patterns for resonant frequencies can be seen.

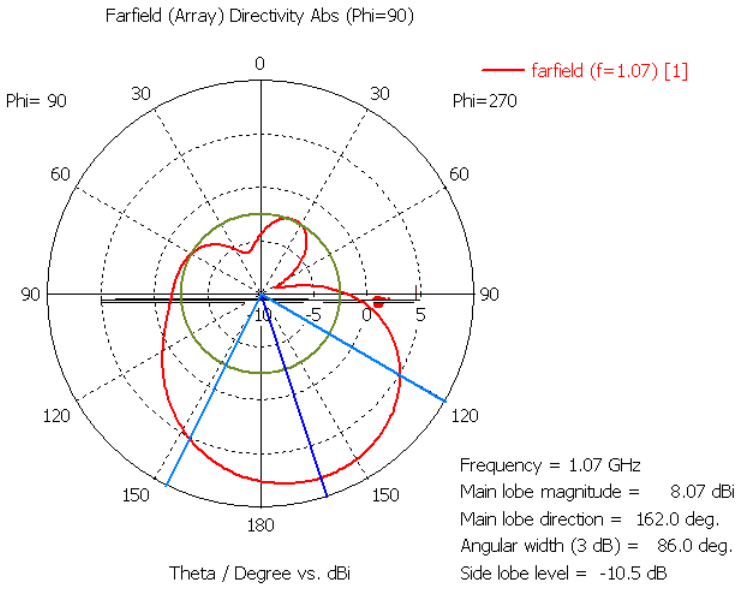

Figure 11: Farfield plot of 1.07 GHz.

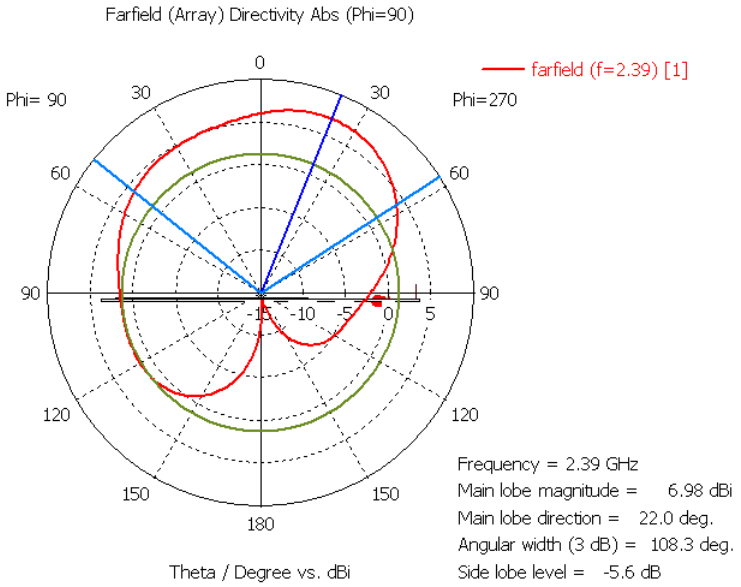

Figure 12: Farfield plot of 2.39 GHz.

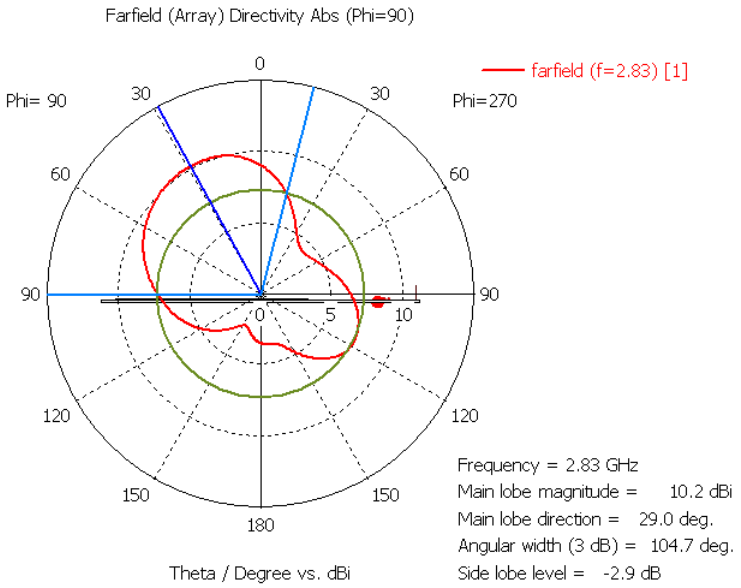

Figure 13: Farfield plot of 2.83 GHz.

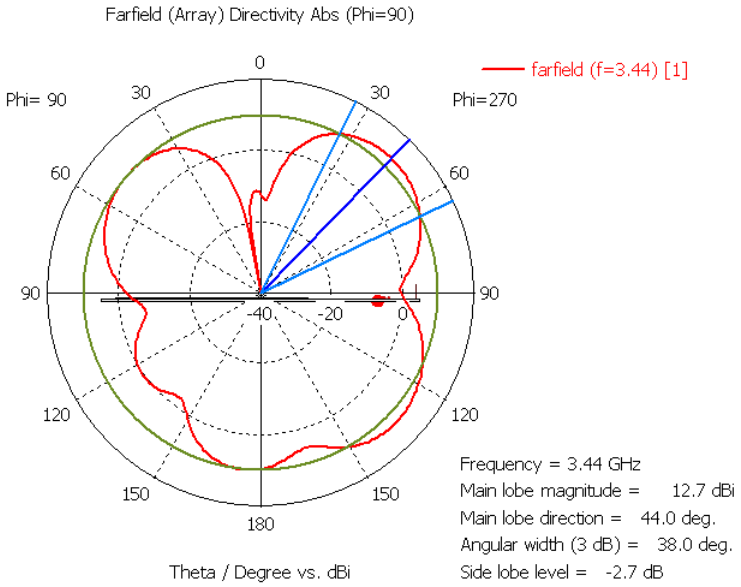

Figure 14: Farfield plot of 3.44 GHz.

The directivity of the antennas in each mode is 8.07 dBi, 6.98 dBi, 10.2 dBi, and 12.7 dBi, respectively. Gain values which are obtained from CST software states that from lowest to highest frequencies are 2.87 dBi, 9.04 dBi, 0.072 dBi and 4.21 dBi.

The patterns for radiation can be altered by applying a shift in phase in each port. Because it will be used in context of communication, having an antenna with directive pattern could not be favorable. Additional equipment can be applied to the mechanical design such as reflector panels behind the antenna, to ensure pattern is radiated in one direction.

4.3 mmWave Patch Antenna

As mentioned earlier, it is a miniaturized version of the sub-6 GHz antenna. Thicknesses for copper and FR-4 substrate were kept constant. The dimensions of the patch can be obtained in the next section.

4.3.1 Dimensions of mmWave Antenna

The width of the patch is 3.6 mm while the length is 4.32 mm. Copper is used again, with a thickness of 0.035 mm. Slot dimensions are 1.73 mm wide and 0.32 mm long, with distance from each other is 0.72 mm. The first slot starts from the top of the patch by 0.288 mm. The T-junction was recreated according to not 50Ω but 70Ω due to low simulation results. The thickness of the feeding line is 0.725 mm, while the junction width is 0.363 mm.

Back of the plate houses the ground plane, where from bottom it has a length of 6.28 mm. The dimensions for the meandered section of the ground are illustrated in the figure below. The cuts are 1.05 mm above the bottom and have separation of 0.72 mm in between them. Center orientation is applied again.

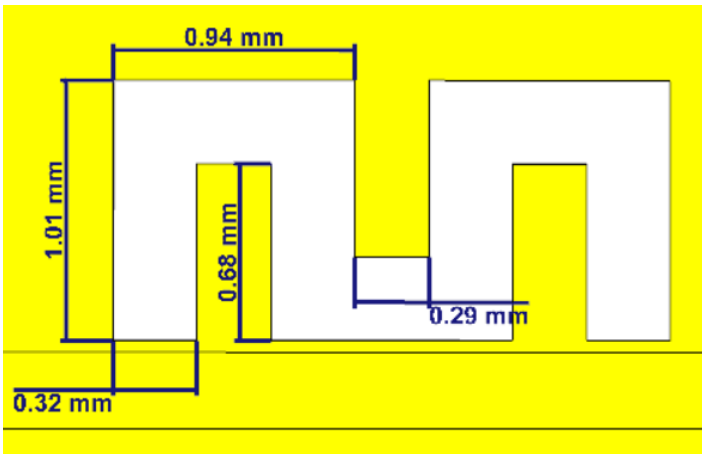

Figure 15: Dimensions of the meandered ground of mmWave.

4.3.2 Results of mmWave Antenna

This antenna is a single resonant frequency antenna unlike the previous design. It resonates at the peak value of 35.09 GHz. This frequency lies in the range of mmWave frequencies.

4.3.3 S11/Return Loss of mmWave Antenna

A graph is presented to show the value of return loss.

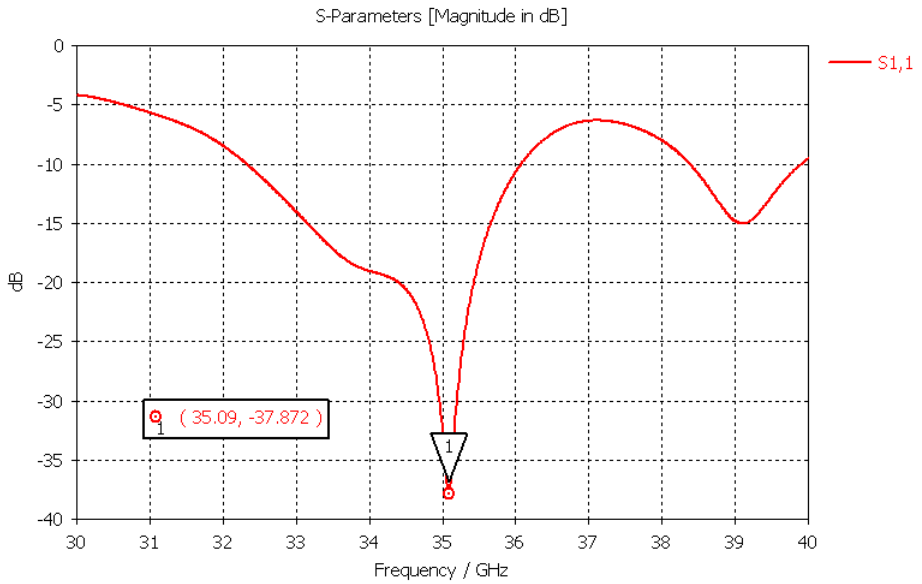

Figure 16: S11 parameters for mmWave antenna.

-10 dB bandwidth of this signal is 3.73 GHz, ranging from 32.34 GHz to 36.07 GHz. This is a very wide coverage on the center frequency.

4.3.4 Radiation Pattern of mmWave Antenna

Radiation pattern is observed at the center frequency of the antenna. The figure below shows the formation below.

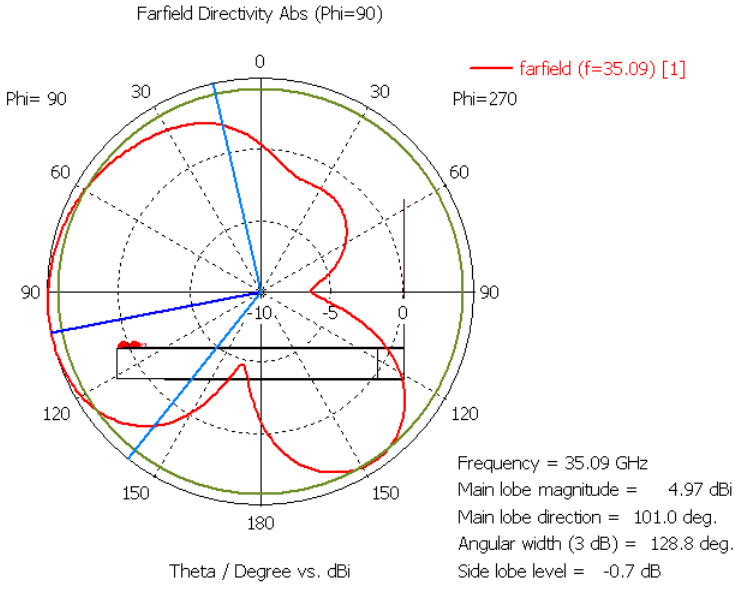

Figure 17: Radiation pattern of mmWave antenna.

The directivity value of the antenna is found to be 4.97 dBi. The gain value of the antenna is found to be 1.81 dBi.

4.4 Array Formats

With the help of the CST software's built-in array factor function, achieving far field results for a designed antenna system is possible without needing to repetitively be copying the same design over and over.

Because the project revolves around the MIMO concept, not all the antennas need to be connected by a single microstrip line. Members of two antennas were selected to be a part of an array, thus making multiple port connections to each antenna via cables when produced.

4.4.1 Sub-6 GHz Antenna Array

The array format of sub-6 GHz antenna was selected to be four of these antennas placed on top of each other. In y-direction, distance between each member is selected to be 70 mm. Resulting far field patterns can be observed in the figures.

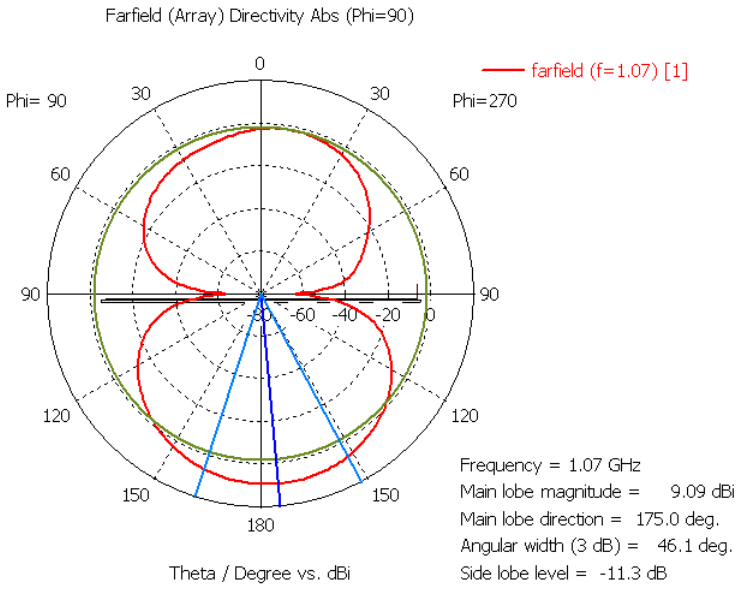

Figure 18: Farfield plot of sub-6 GHz array at 1.07 GHz.

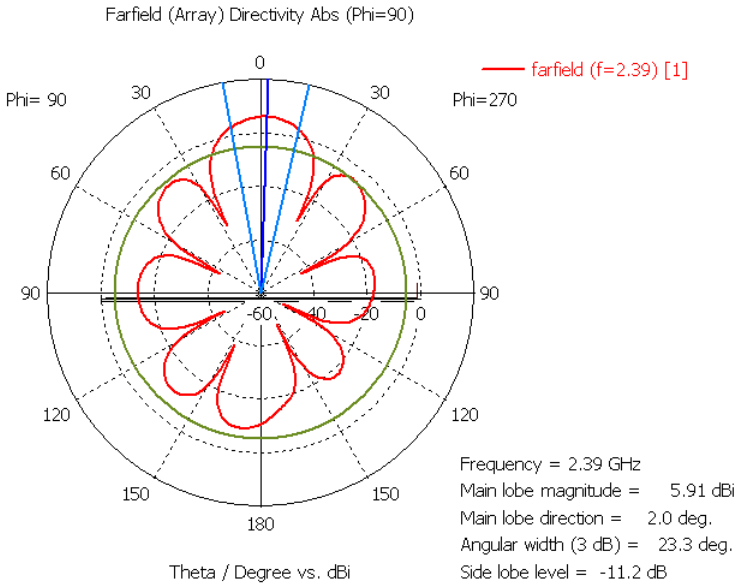

Figure 19: Farfield plot of sub-6 GHz array at 2.39 GHz.

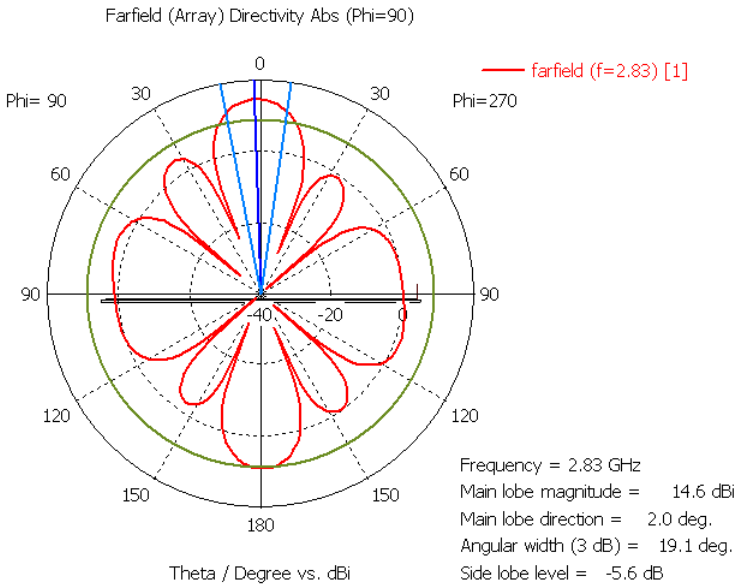

Figure 20: Farfield plot of sub-6 GHz array at 2.83 GHz.

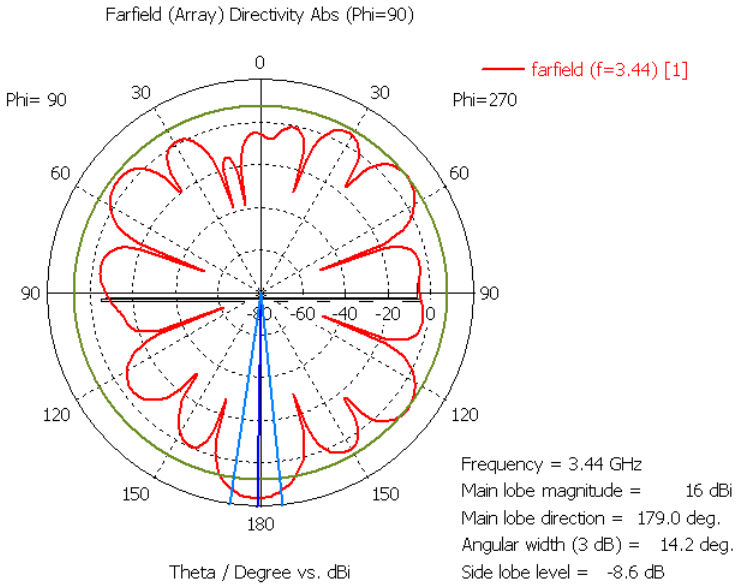

Figure 21: Farfield plot of sub-6 GHz array at 3.44 GHz.

As the members increase, it can be observed that the beamwidth gets narrower, and there is an increase in gain and directivity. Many side lobes are generated for most of the frequencies above, which will also help in propagating the signals when mounted.

In order from low to high frequencies, obtained directivity values are 9.09 dBi, 5.91 dBi, 14.6 dBi, and 16 dBi. The gain values corresponding are 1.96 dBi, 10.2 dBi, 4.39 dBi, and 7.45 dBi.

4.4.2 mmWave Antenna Array

For mmWave, again four elements were used with spacing of 5 mm in between array members. The resultant far field graph is generated.

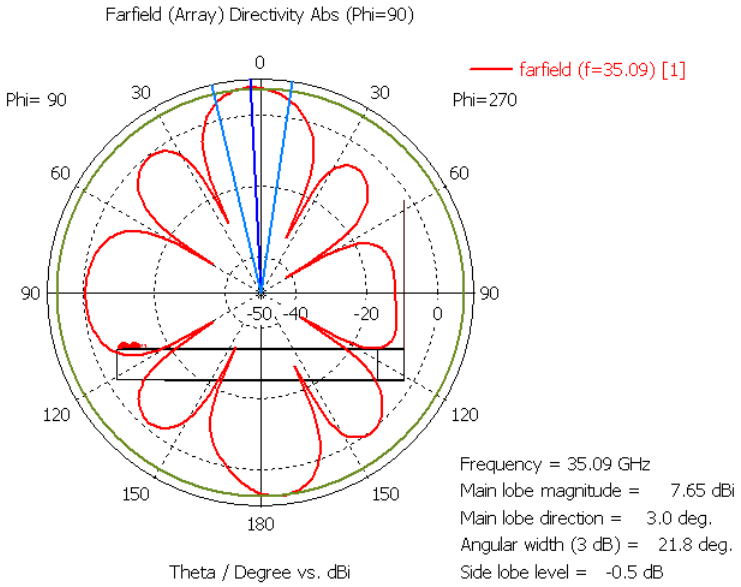

Figure 22: Farfield plot of mmWave array at 35.09 GHz.

It can be seen from the graph that by turning the singular antenna element into an array form shifts the main beams direction from –101 degrees to 3 degrees. Directivity and the gain values are 7.65 dBi and 4.5 dBi, respectively.

4.5 Comments and Comparison

To make comments about the values and the graphs obtained, a table of all the values will be presented below.

Table 1: Parameters of single sub-6 GHz antenna.

Parameter	1.07 GHz	2.39 GHz	2.83 GHz	3.44 GHz
Return loss (dB)	-15.87	-15.61	-17.94	-18.24
Directivity (dBi)	8.07	6.98	10.2	12.7
Gain (dBi)	2.87	9.04	0.072	4.21
Lobe width (deg)	86	108.3	104.7	38
Bandwidth in MHz	30.3	40.7	51.3	68.2

Table 2: Parameters of single mmWave antenna.

Parameter	35.09 GHz
Return loss (dB)	-37.87
Directivity (dBi)	4.97
Gain (dBi)	1.81
Lobe width (deg)	128.8
Bandwidth in MHz	3732

Table 3: Values obtained from sub-6 GHz array.

Parameter	1.07 GHz	2.39 GHz	2.83 GHz	3.44 GHz
Directivity (dBi)	9.09	5.91	14.6	16
Gain (dBi)	1.96	10.2	4.39	7.45
Lobe width (deg)	46.1	23.3	19.1	14.2

Table 4: Values obtained from mmWave array.

Parameter	35.09 GHz
Directivity (dBi)	7.65
Gain (dBi)	4.5
Lobe width (deg)	21.8

When in array format, the general trend is increase in gain and directivity but decrease in lobe width. There are some exceptions such as directivity decrease in 2.39 GHz and gain decrease in 1.07 GHz.

Overall, compared to previous works carried out in the same context, the values obtained are agreeable. In [2], the return loss parameters of the designed antenna show around -30 dB range peak values in array form at the resonant frequencies, while in this design, the values obtained are in the range of -15 to -18 dB just for a single element of array. The reason for this twice the increase in gain in dB-wise is that adopting reflector panel addition in their design. As said earlier, reflector panels increase the bandwidth and decrease back lobes, the return loss can increase

proportionally. The return loss values for the array of sub-6 GHz antenna working at a single frequency shows minimum of -45 dB. The graph of this single tested variable is available in the appendices section. The reason for S11 values of array formatting not fully available is that the CST program is a heavy program that takes too much time to simulate if the computer is old.

The radiation patterns of the current design compared with [1] shows similar outcomes. When [1] and [2]'s radiation patterns are compared, the patterns of [2] show almost only front lobes, while the patterns of this design and [1] are bi-directional. The usage of the antennas is for two different applications.

The general comparisons between the selected two papers are that the return loss values increase drastically when put in array form which corresponds to agreed values in between these articles also for common sense. The same trend is observed in the current design. Increase in return loss parameters and directions of the radiation patterns are somewhat agreed to be correct and project is yet nearly to be finalized.

Chapter 5

CONCLUSION AND FUTURE WORK

5.1 Conclusion

In conclusion, two sets of antennas are designed and tested electronically. Both antennas are capable of being set up in any format making them an array and having freedom to connect them separately creates the MIMO interface. The frequency ranges stated above cover the bands that are and will be used when 5G networking becomes global. Comprehensive simulations are carried out and the validations seem to be in the range of an acceptable antenna's parameters. Many of the parameters obtained and compared with similar work. The said antenna design can not only be used in base station but for home reception antennas as well. The system can be set up for North side of Cyprus to allow the 5G signals to be distributed in addition to the current base station antennas. Using the antennas in array format strongly boosts the said parameters discussed earlier.

5.2 Future Work

For the future work, beam steering technique should be tested, as it can be achieved by changing the phase of the signal in each port. This kind of process requires more time and computational power, as the simulation times become longer as the system becomes more complex. Using a high-power computer could resolve this problem.

Effects of transmission lines on the antenna performance should be observed, as the length of the strip line changes the phase induced on the antenna.

Fabrication of a prototype can be thought to carry out field testing. That way, comparison between simulation and real-life values could be completed.

Antenna housing should be produced, elements such as a radome or a reflector panel could be added to protect the antenna or to decrease back lobes generated.

REFERENCES

[1] Chang, C., & Chen, Y., (2016). Design of a four-element multiple-input–multiple-output antenna for compact long-term evolution small-cell base stations. *IET Microwaves, Antennas & Propagation*, doi:10.1049/iet-map.2015.0540.

[2] Cui, Y., Li, R., & Wang, P., (2013). Novel Dual-Broadband Planar Antenna and Its Array for 2G/3G/LTE Base Stations. *IEEE Transactions on Antennas and Propagation*, 61(3), 1132–1139., doi:10.1109/TAP.2012.2229377.

[3] Errifi, H., Abdennaceur, B., & Badri, A., (2014). Design and Simulation of Microstrip Patch Array Antenna with High Directivity for 10 GHz Applications. Retrieved from https://www.researchgate.net/publication/309673437_Design_and_Simulation_of_Microstrip_Patch_Array_Antenna_with_High_Directivity_for_10_GHz_Applications

[4] Moradi, K., & Nikmehr, S., (2012). A Dual-Band Dual-Polarized Microstrip Array Antenna for Base Stations. *Progress In Electromagnetics Research*, 123(), 527–541., doi:10.2528/PIER11111610

[5] Huang, Y., Boyle, K., (2008), *Antennas: From Theory to Practice*

[6] Bird, T., (2009). Definition and Misuse of Return Loss. *IEEE Antennas and Propagation Magazine*, 51(2), 166–167., doi:10.1109/map.2009.5162049

[8] Floyd, T., (1997). Principles of Electric Circuits (5th ed.), Prentice Hall, ISBN 0-13-232224-2

[9] Antenna Theory – Radiation Pattern, Tutorials Point. Retrieved from https://www.tutorialspoint.com/antenna_theory/antenna_theory_radiation_pattern.htm

[10] Dragan, P., Mario C., (2019). Human Interaction with Electromagnetic Fields.

[11] What is antenna polarization, Trelink. Retrieved from https://www.trelink.com/what-is-antenna-polarization/

[12] Haupt, R. L. (2010). Antenna arrays, a computational approach. Pennsylvania State University, John Wiley & Sons, Inc., 2010.

[13] Albreem, M., Juntti, M., & Shahabuddin, S., (2019). Massive MIMO Detection Techniques: A Survey. *IEEE Communications Surveys & Tutorials*., doi:10.1109/COMST.2019.2935810.

[14] MIMO (multiple input, multiple output), SearchMobile Computing – TechTarget. Retrieved from https://searchmobilecomputing.techtarget.com/definition/MIMO

[15] Junjun, W., Lecture on Antenna Theory and Design, *School of Electronic and Information Engineering*, Chapter 5. Retrieved from

http://is.buaa.edu.cn/__local/2/B0/12/A9B46CAD1CEDF3E8A85EB82C7F7_1E368AA5_2EEE0C.pdf.

[16] Dafalla, Z., Kuan, W., Rahman, A, Shudakar, S., (2004). Design of a rectangular microstrip patch antenna at 1 GHz, *IEEE 2004 RF and Microwave Conference*. (0), 145–149, doi:10.1109/rfm.2004.1411097

[17] Roy, B., Bhattacharya, A., Bhattacharjee, A., Chowdhury, S., (2015). Effect of different slots in a design of microstrip antennas. *IEEE 2015 2nd International Conference on Electronics and Communication Systems*. (), 386–390., doi:10.1109/ECS.2015.7124931

[18] Douville, R., James, D., (1978). Experimental Study of Symmetric Microstrip Bends and Their Compensation., 26(3), 175–182., doi:10.1109/tmtt.1978.1129340

[19] Microstrip Miter Bend Calculator, Formula, Equations, RF Wireless World, Retrieved from https://www.rfwireless-world.com/calculators/Microstrip-Mitred-Bend-Calculator.html

[20] Lee, H., Choi, W., (2013), Effect of Partial Ground Plane Removal on the Radiation Characteristics of a Microstrip Antenna, doi: 10.4236/wet.2013.41002

APPENDIX

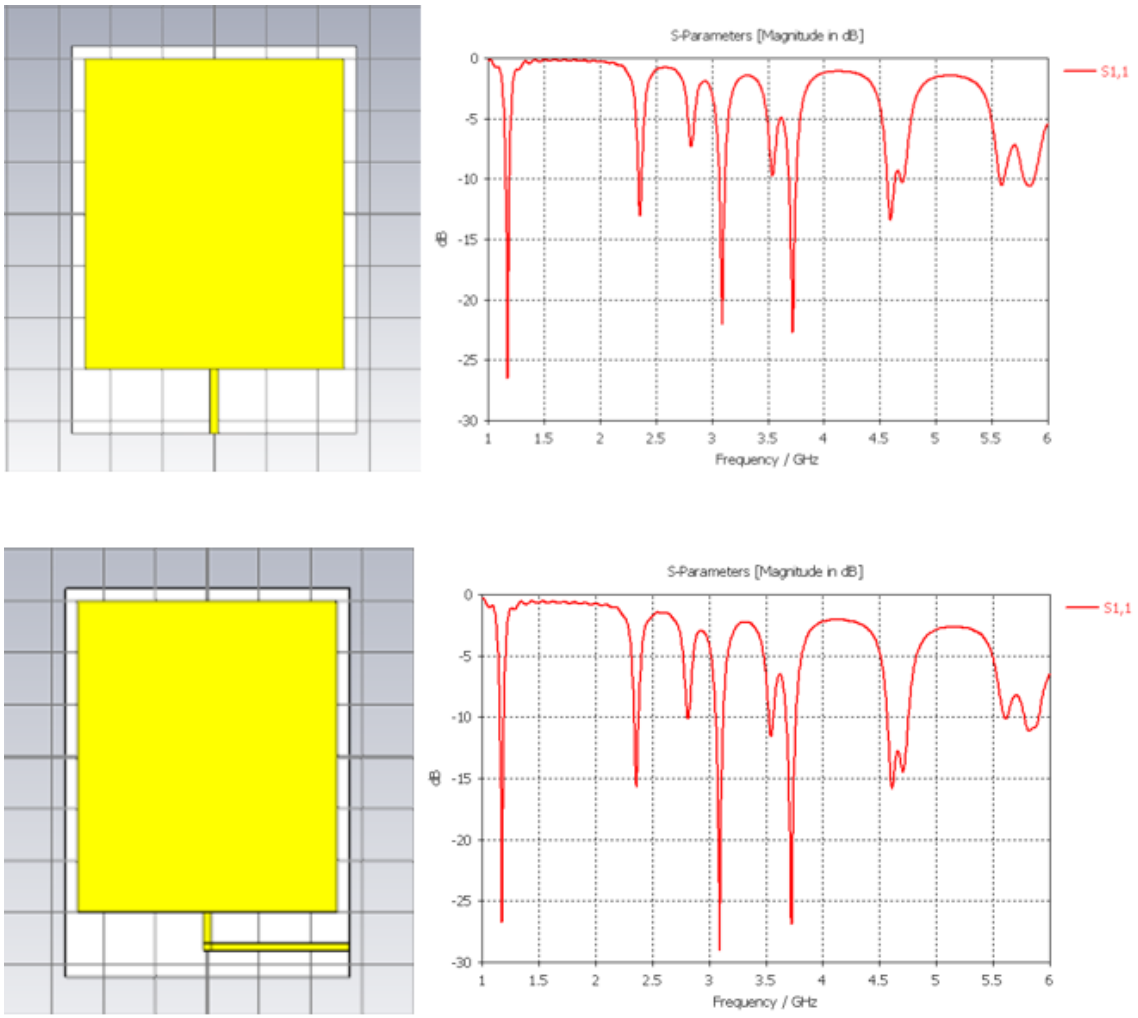

Figure 23: Version 2 and version 3, effect of transmission line length on S11 parameters.

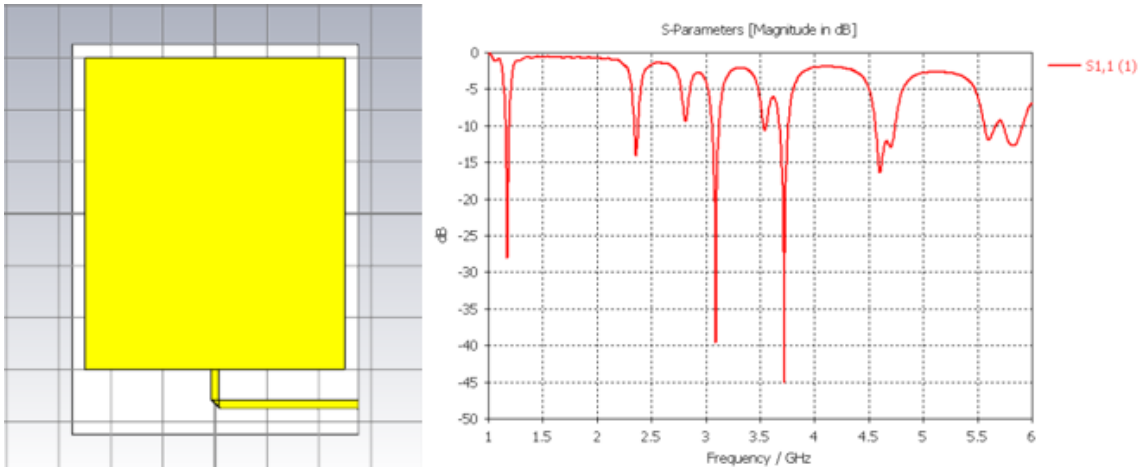

Figure 24: Version 4, effect of miter bend, must be compared with version 3.

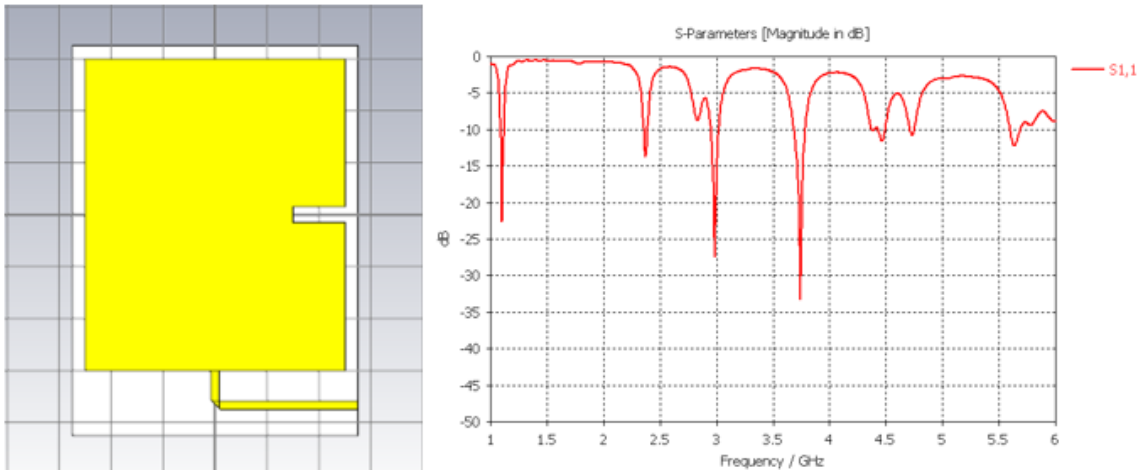

Figure 25: Version 5, effect of slot on patch, must be compared with version 4.

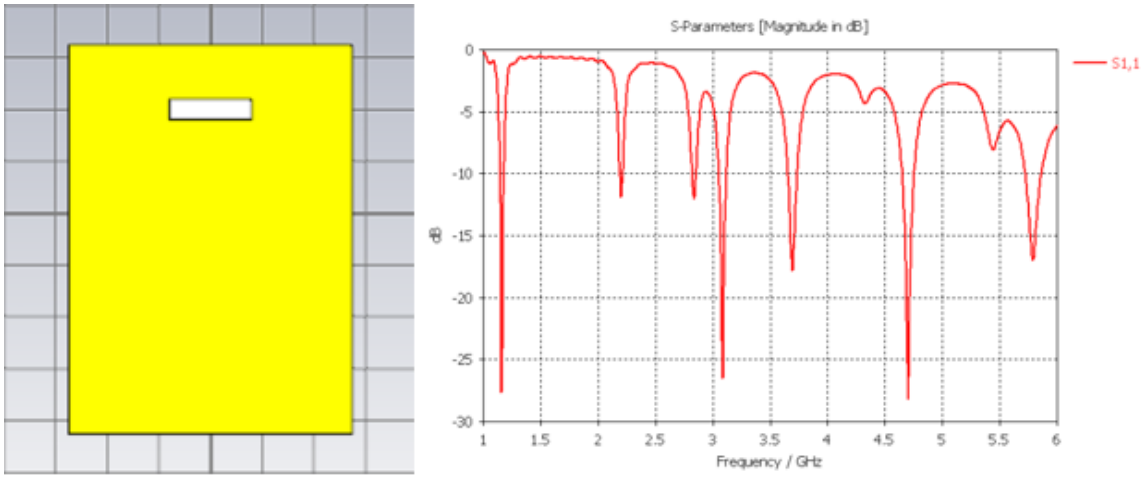

Figure 26: Version 6, effect of slot in ground, must be compared with version 4.

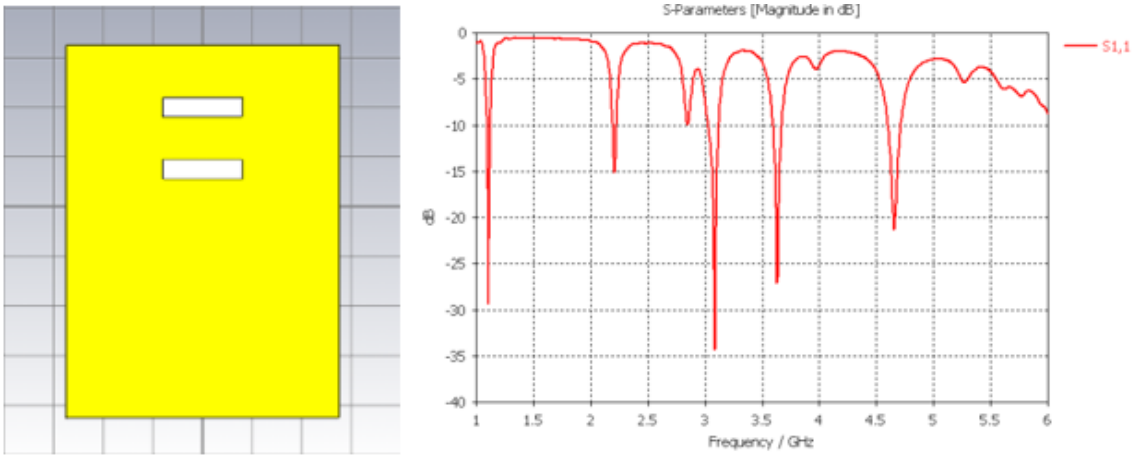

Figure 27: Version 7, effect of double slot in ground, must be compared with version 6.

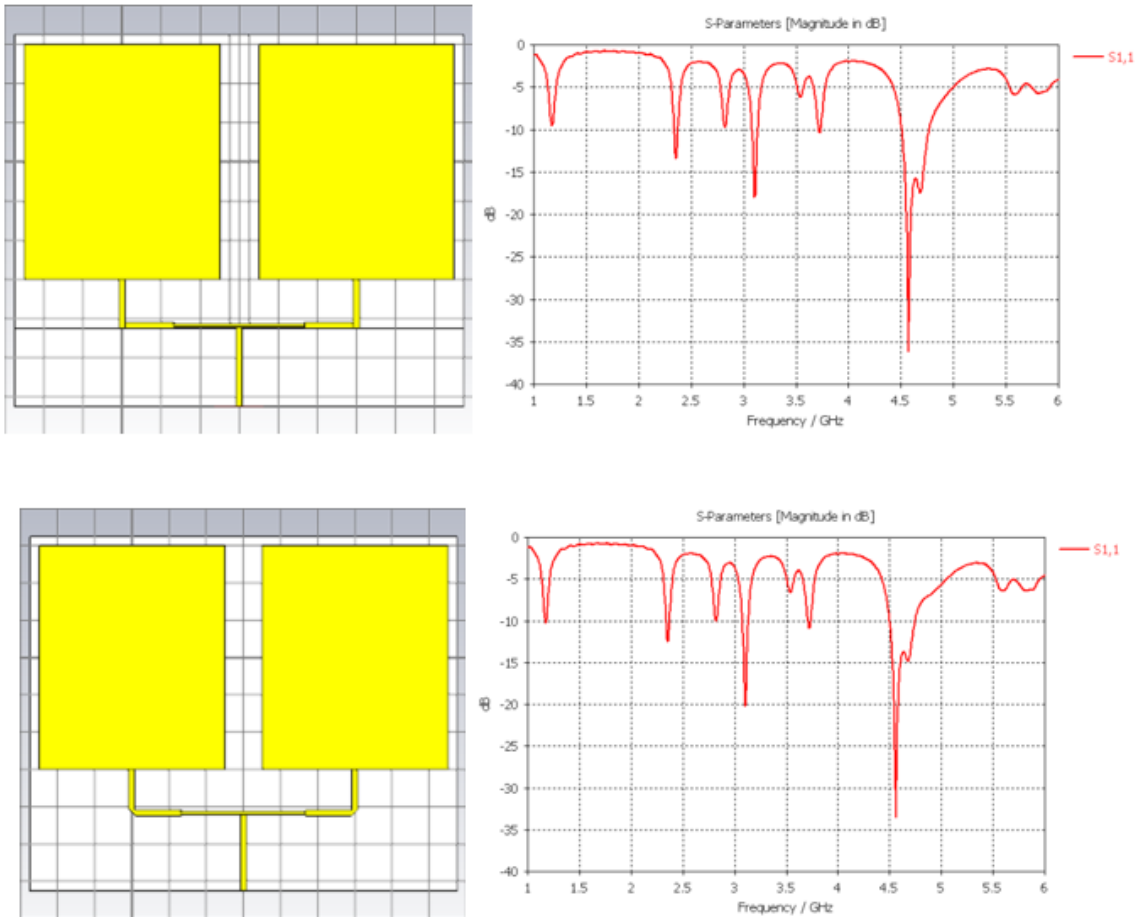

Figure 28: Version 9 and version 11, effect of miter bend on S11 parameters.

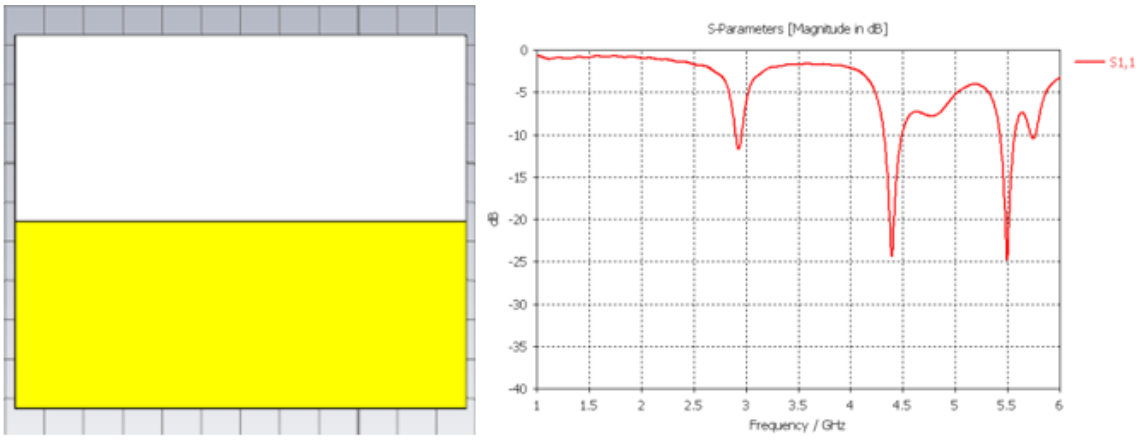

Figure 29: Version 12, partial ground effect, must be compared with version 11.

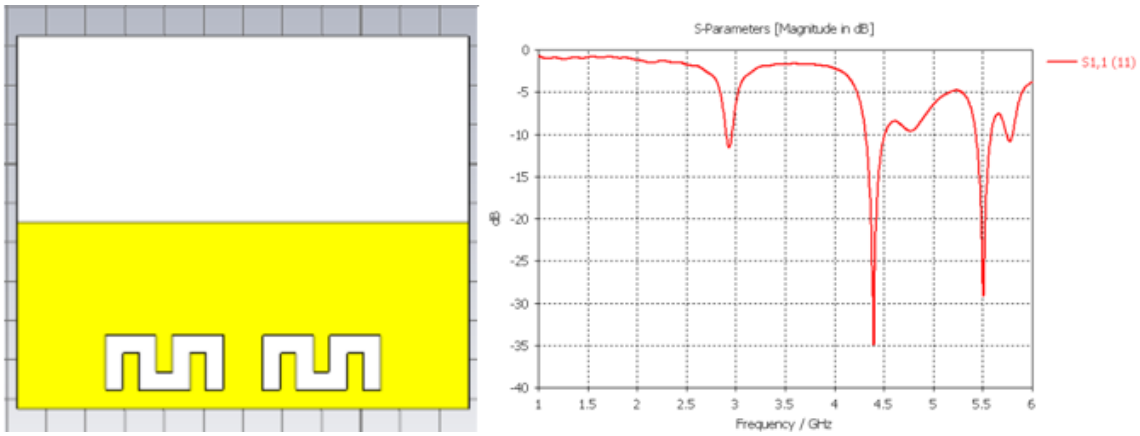

Figure 30: Version 15, meandered ground plane effect, must be compared with version 12.

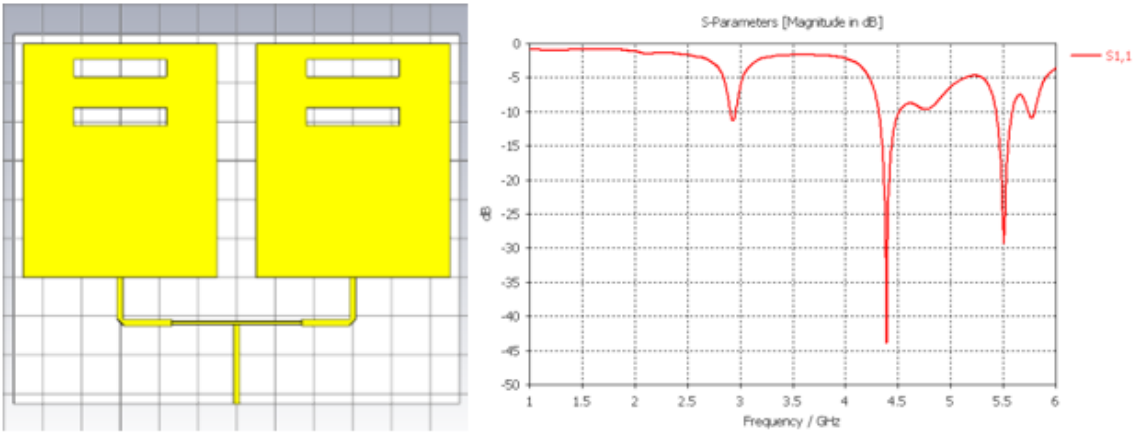

Figure 31: Version 16, effect of double slots on patch, must be compared with version 15.

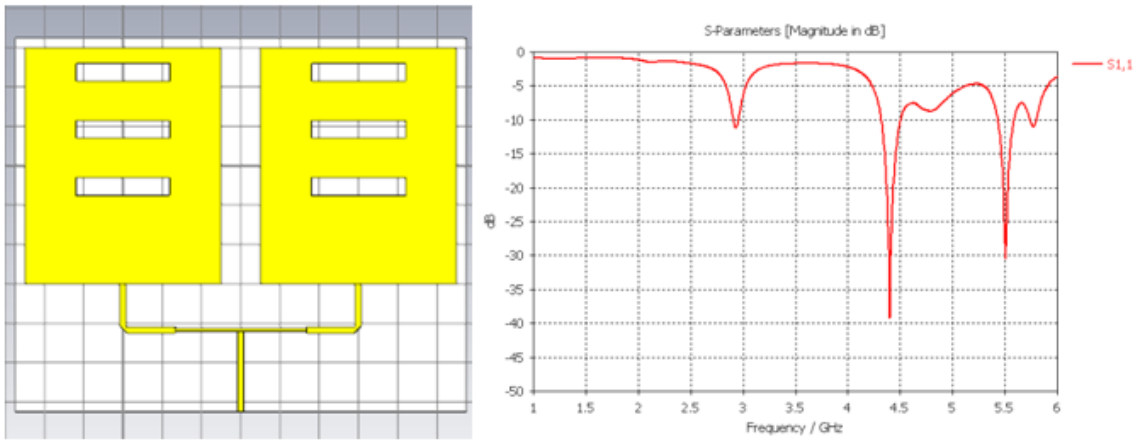

Figure 32: Version 17, effect of triple slots on patch, must be compared with version 16.

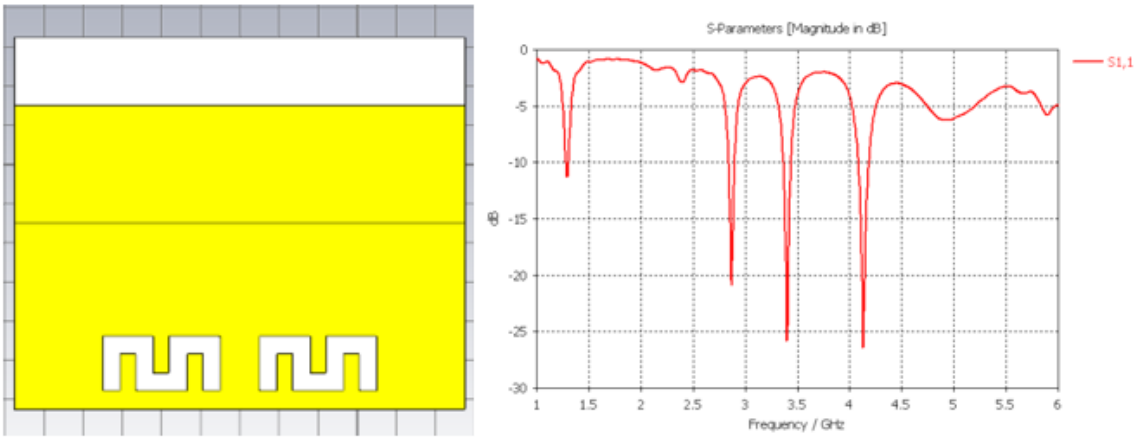

Figure 33: Version 18, effect of additional ground plane introduced, must be compared with version 17.